DOI: 10.15480/882.9321

Eighth International Symposium on Marine Propulsors
smp'24, Berlin, Germany, March 2024

Cavitation Prediction by wake dependent Open-Water Interpolation

Thorsten Tillack[1], Hagen Lippok[1]

[1]SCHOTTEL GmbH, Dörth, Germany

ABSTRACT

This paper describes the development of a post-processing method for a set of steady-state finite volume method results to make a pseudo-transient cavitation prediction for propellers in behind hull condition by interpolation. At the time of writing, predicting the propeller cavitation in behind hull condition requires a time-consuming transient calculation with a dynamically rotating mesh for each operation point under consideration. In order to speed up this process an approach is developed where the solution field of a steady propeller open water performance calculation is rotated in relation to a vessel's wake field. During this rotation, the wake induced shift in the propeller's operation point on each cell of the simulation is used to interpolate over the calculated solutions. This workflow is tested with the known Potsdam Propeller Test Cases for homogeneous and oblique inflow. A good agreement between higher quality computational methods and the calculated prediction is achieved.

Keywords

CFD, Wake Field, Cavitation, Propeller-Hull Interaction

1 INTRODUCTION

The requirements on contemporary propeller designs have been evolving continuously. Larger and faster vessels require a more detailed look into the propeller design. During the propeller design process, predicting the cavitation behaviour is a major concern. Because the evolving requirements push the propeller design and thus the propeller loads towards more extreme points, the demands on the prediction methods rise as well, to a point where traditional methods cannot keep up with the required accuracy. Hence for high loaded applications with a great risk for cavitation the use of RANSE calculations is unavoidable.

Comparing vortex-lattice method (VLM), boundary element (BEM) and RANSE finite volume method (FVM), VLM is the fastest, whereas FVM provides the highest level of detailing. Vortex-lattice methods reduce the entire blade profile to its camber surface and solve the equations on discrete patches. Caused by this approach, VLM is not able to evaluate detailed effects of profile curvature in the propeller's wake and at a distance to the propeller's camber surface. Hence neither a volumetric prediction of cavitation nor a direct simulation of the tip vortex is possible. FVM on the other hand, resolves the propeller surface as well as the surrounding flow and can thereby predict volumetric effects like vortices and cavitation. This may be done by simulating the phase transition using two-phase flow (e.g. VOF) with a cavitation model (e.g. Schneer & Sauer 2001) which gives the actual vapour regions.

One drawback of FVM simulations which resolve cavitation is the necessary calculation time, which makes a rapid review of multiple operation points for every propeller design iteration impossible. Although a steady-state propeller open water curve (OWC) is available within 3-5 hours with a reasonable amount of hardware resources, especially transient cavitation calculations in behind hull condition will take several days.

Scaling down the requirements on the calculation and reverting to single phase simulations can help reduce the calculation time. In general, cavitation occurs if the local pressure drops below the vapour pressure of the fluid, leading to a phase transition. For predicting cavitation inception with FVM it is sufficient to check the pressure field within the simulation's solution for values below the vapour pressure.

A relatively quickly to compute steady-state calculation to determine the propellers open water performance already contains the required pressure information to determine the cavitation risk for the advance ratio J of that calculation. J combines, as Equation (1) shows, the advance speed V_a of the system with the propeller speed n and propeller diameter D.

$$J = \frac{V_a}{(n \cdot D)} \tag{1}$$

Hence a prediction of the cavitation risk for a specific advance ratio is possible by only using the pressure information and detecting regions with local values below vapour pressure in the pressure field.

In behind hull condition, the propeller is subject to a non-uniform inflow described by the wake field. As a result, different parts of the propeller operate at different local operation points at different points in time. This transient behaviour cannot be simulated by a single steady-state calculation or even multiple calculations at different operation points. The interpolation of several open water calculations for different advance ratios at a specified operation point considering the wake field and thus the local change in the propeller's inflow condition solves this limitation.

2 METHODS

The methods compared in this study are the vortex-lattice method, the boundary element method, the finite volume method and the newly developed wake-dependent interpolation. First, an overview of the used software packages implementing the existing methods is given, followed by the description of the newly developed wake-dependent interpolation.

2.1 Software Packages

2.1.1 Vortex-Lattice Method

VORTEX 2020 is an implementation of the vortex-lattice method developed by SVA Potsdam, with a propeller surface cavitation prediction done by CAVIPLOT (Schulze 1995). VORTEX determines the blade load for a given discretization of the blade and the combined open water curve for the entire blade. This calculated blade load distribution on the camber surface of the blade is then compared against the local vapour pressure and visualized using CAVIPLOT.

2.1.2 Boundary Element Method

MPUF/PROPCAV version R2019 was developed by the University of Texas (Kinnas et al 2003). PROPCAV is a BEM solver based upon the well-known MPUF developments.

2.1.3 Finite Volume Method

HELYX-Core v.3.2.0 is an OpenFOAM based, incompressible, isothermal, single phase FVM solver distributed by Engys. The coupled pressure-based solution algorithm solves the governing Navier Stokes equations.

$$\nabla \cdot \vec{u} = 0 \tag{2}$$

$$\nabla \cdot (\vec{u}\vec{u}) = -\frac{1}{\varrho}\nabla p + \nabla \cdot [\nu_{eff}(\nabla \vec{u})] \tag{3}$$

with the volume velocity vector field $\vec{u}$, the density ϱ, the pressure p and the combined laminar and turbulent kinematic viscosity ν_{eff} (Mangani et al 2014). Turbulence is modelled with RANS k-ω-SST and an all y^+ wall treatment wall model reaching a mean CFL number of ~120. Time discretization is first order and the boundary conditions are set to velocity inlet and pressure outlet. The meshes are unstructured hexahedral dominated meshes with around 10 boundary layers and an ensured coverage of >90% on the blades.

2.2 Wake-dependent Interpolation

The proposed wake-dependent interpolation is based on a FVM calculated set of advance ratios within a suitable range around a specific operation point without any modification of the inflow to the propeller ("open water condition").

2.2.1 Calculation Set

At least two FVM calculations are necessary to interpolate the results. The more calculations are made the better the quality of the interpolation, as higher order interpolation schemes such as cubic spline interpolation become available. Checking the wake field for maximum and minimum change of local advance ratio gives the minimum and maximum advance ratio that should be calculated to correctly interpolate the results without the danger of extrapolating at extreme wake deviations.

One calculation mesh must be used for all calculations so that the cells of each solution perfectly align and differences in the meshes cannot influence the quality of the interpolation. This necessitates the generation of a compromise mesh, especially regarding the boundary layers, because a wide range of advance ratios may need to be covered in a sufficiently accurate way.

Much like model tests are performed at parameters (advance speed, propeller speed) not necessarily corresponding to the full-scale operation point but at an equivalent operation point, the calculations can be performed at an arbitrary operation point and due to equivalence all possible operation points in full-scale can be interpolated from the calculation set. To facilitate this, it is essential that all solution fields that will be interpolated (the pressure field in the case of cavitation inception) are first made dimension-less by using a conversion analogous to the well known thrust coefficient K_T given in Equation (4),

$$K_T = \frac{T}{\varrho n^2 D^4} \tag{4}$$

where T is the thrust, ϱ the density of water, n the propeller speed and D the propeller diameter. The conversion for the pressure result p would thus be according to Equation (5).

$$K_p = \frac{p}{\varrho n^2 D^2} \tag{5}$$

It is this pressure coefficient that will be interpolated, and which needs to be transformed back to a pressure with the parameters of the operation point under survey. For brevities sake going forward we will write about "interpolating the pressure" but imply this conversion.

2.2.2 Wake Field

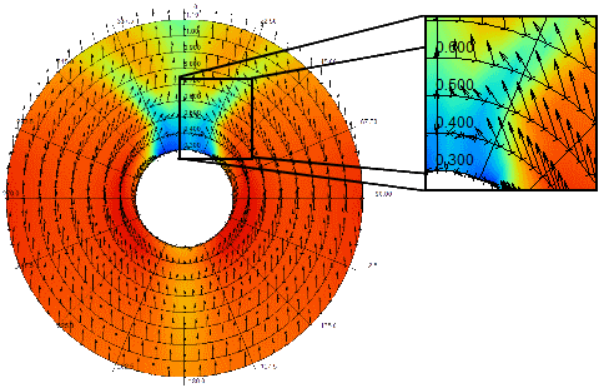

Figure 1 Example wake field [color: axial component / tangential and radial represented as resulting vector]

A wake field, as shown in Figure 1, describes local changes of axial, tangential and radial velocity components at different points in the propeller plane as ratios of the advance speed as given in Equation (6).

$$v_x = \frac{v_{ax}}{V_a}$$
$$v_t = \frac{v_{tan}}{V_a} \qquad (6)$$
$$v_r = \frac{v_{rad}}{V_a}$$

While each FVM calculation is done at a specific advance ratio J according to Equation (1), each location in the wake field modifies this J to a J_{local}.

Using the advance speed of the calculation, the actual axial velocity at each point in the wake field can be calculated with Equation (7).

$$v_{ax,actual} = V_a \cdot v_x \qquad (7)$$

Going further, the tangential component of the wake field v_t is used to compute the hydrodynamic rotation speed of the propeller given in Equation (8),

$$n_{hyd} = (v_t \cdot V_a + \omega r)/(2\pi r) \qquad (8)$$

where ωr is the tangential speed at the radius r. This accounts for a virtual shift in propeller speed due to accelerated or decelerated tangential inflow into the propeller. Combining both influences yields the local advance ratio J_{local} for each point in the wake field as shown in Equation (9).

$$\mathrm{J_{local}} = \frac{v_{ax,actual}}{(n_{hyd} \cdot D)} \qquad (9)$$

Currently the propeller induced influence on the wake field itself is not considered. Goldstein factors (Goldstein, 1929) or more modern approaches could be incorporated in the local evaluation of the wake field to represent this aspect and further improve the prediction.

2.2.3 Interpolation

Using the same FVM mesh for all calculations in the set ensures that the cells and the result values for different solution fields of the mesh stay at the same location between calculations, regardless of the advance ratio. It is thus easy to construct an interpolation for each cell over all calculated advance ratios.

Each cell of the FVM mesh has a centroid coordinate that can be mapped onto the wake field by determining its radial and angular position in relation to the rotation axis of the propeller. Thus, the local advance ratio can be obtained from the wake field and the cell's interpolation of the pressure result be evaluated, yielding the interpolated pressure $p_{interpol.}$ at each specific point.

To simulate the rotation of the propeller in the wake field, each centroid coordinate is rotated by the same angle in the desired direction and the wake field evaluated again. Stringing these rotations together gives the opportunity to evaluate a complete revolution of a propeller in a wake field.

The interpolation is not limited to pressure results. Any results obtained from the FVM calculations can be interpolated by this method.

2.2.4 Cavitation Inception

To determine if cavitation occurs at a cell the local pressure is calculated as shown in Equation (10), where p_{atm} is the atmospheric pressure at sea level (typically $p_{atm} = 101325$ Pa) and the last term the influence of the immersion depth of each individual cell in the solution field.

$$p_{local} = p_{interpol.} + p_{atm} + \rho_{water} \cdot g \cdot h_{sp} \qquad (10)$$

Cavitation is likely to occur if p_{local} is below vapor pressure which is $p_v = 1670$ Pa in the context of this paper. A precise determination of the cavitation type is not possible.

2.2.5 Performance Considerations

The interpolation does not necessarily need to be executed for the whole FVM mesh. A typical mesh for a simulation has around $12 \cdot 10^6$ to $16 \cdot 10^6$ cells. While many of these cells are near to or at the propeller, some are farther out in the computational domain where the wake field does not correctly represent flow conditions. To keep interpolation time low, it is prudent to interpolate over only a subset of cells of the original solution.

Different subsets of cells are conceivable. For a survey of just the propeller's surface and no volumetric information about the cavitation it is sufficient to interpolate only over all boundary patches of the mesh, even discarding all boundary layers. This typically reduces the data set to about $500 \cdot 10^3$ cells and is very quickly done. If a volumetric evaluation is desired a selection of only the cells within $1D$ of the propeller's centre will give a slightly reduced cell count and discard cells that will not be influenced correctly by the wake field. Because of the boundary layers still being present, this subset will still be fairly large.

A more efficient reduction of cells can be achieved by creating a second, coarser mesh with a smaller spatial extent than the original one (e.g. $1D$ around the propeller's centre), perhaps different cell sizes and/or transition

between cell sizes and no boundary layers. A mesh like this might consist of around $2 \cdot 10^6$ cells. By mapping the calculation results onto this smaller mesh, a certain amount of interpolation between cells will already take place but given a carefully constructed smaller mesh the error introduced by mapping the results can be negligible in view of the desired qualitative observation of cavitation inception.

3 TEST CASES

The method of wake-dependent interpolation is tested on the propeller of the PPTC of SVA Potsdam (SVA Potsdam 2011, SVA Potsdam 2015). The propeller geometry and model test data are publicly available. Table 1 shows the main parameters for the propeller and Table 2 shows the propeller design parameters and the operation point.

Table 1 Propeller main parameters for VP1304

D	Pitch $r/R = 0.7$	Area ratio	Skew	Z
250 mm	1.635	0.779	18.9 °	5

Table 2 Propeller operation point

J	K_T	n	σ_n
0.994	0.387	24.987 rpm	2.024

Because the actual model test is taken as a reference for testing wake-dependent interpolation it is sufficient for any FVM calculation to only model the propeller in model scale. Scaling the results to full scale is not needed.

The propeller is designed to show a pronounced cavitation behaviour at the test operation point, especially a cavitating tip-vortex, so although the different methods are expected to vary in their results cavitation should be predicted in all cases. While the model test does not show sheet cavitation at the leading edge all FVM calculations of the test have shown sheet cavitation at the leading edge (Krasilnikov 2019, Kimmerl et al 2021, Viitanen et al 2020). This seems to be an issue specific to the model test of the PPTC 2011 because model tests have been predicted adequately time and again by using FVM approaches. The comparison of the different methods will therefore be limited to numerical approaches with a two-phase LES set as the solution of best quality.

3.1 Calculation Meshes

Each method has its own calculation mesh. Figure 2 gives a visual overview of the propeller itself and the method's meshes.

(a) 3D rendering of PPTC propeller VP1304 (SVA, 2011)

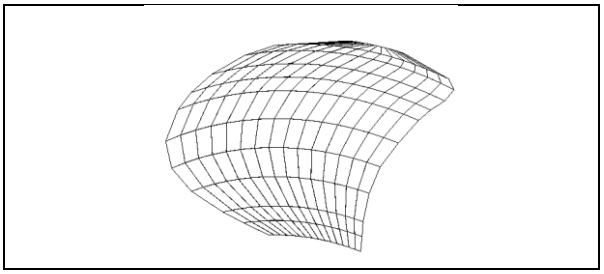

(b) User meshing for VLM

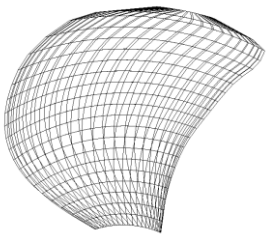

(c) Propeller meshing for BEM calculation

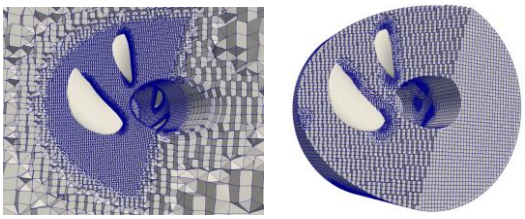

(d) CFD mesh for OWC-calculation / smaller subset mesh for cavitation interpolation

Figure 2 Comparison of geometry discretization

The parameters of the meshes are given in Table 3. For VLM the standard approach is based on the radial resolution of the propeller geometry (e.g. 12 distinctly defined radii and thus 11 elements in radial direction) and 15 elements in chordwise direction. For BEM a resolution of 20 elements in radial and 25 elements in chordwise direction is found to give reasonable results.

Table 3 Comparison of blade discretisation

	Element count per blade	Domain size
VLM	180 - 240 faces	
BEM	1000 faces	
FVM	$1.9 \cdot 10^6$ cells	$20 \cdot D$ in length $10 \cdot D$ in diameter

As BEM resolves the suction and pressure side, a total of 1000 patches describe each blade surface with the patches for hub and the propellers wake excluded. For the FVM propeller meshing the blade surface is resolved with a first cell height of $1 \cdot 10^{-5}$ m, the hub and shaft geometry with $5 \cdot 10^{-5}$ m growing with an expansion ratio of 1.25. Only considering the resulting mesh size FVM is expected to deliver the most accurate results.

3.2 Open Water Performance

Prior to evaluating the different cavitation prediction capabilities, a quick survey of the general calculation accuracy is given. As cavitation is strongly dependent on the load on the blade, an accurate prediction of the thrust and torque characteristics of the propeller is the basis for a reasonable prediction of cavitation risk.

Table 4 Comparison of thrust coefficient for different methods

J	K_T PPTC	VLM	BEM	FVM
0.85	0.488	2.0 %	-1.3 %	1.2 %
0.95	0.432	2.3 %	-1.6 %	1.2 %
1.02	0.394	2.1 %	-1.5 %	1.4 %
1.05	0.377	1.9 %	-1.2 %	1.6 %

Table 5 Comparison of torque coefficient for different methods

J	$10K_Q$ PPTC	VLM	BEM	FVM
0.85	1.153	0.7 %	-1.2 %	0.7 %
0.95	1.050	0.5 %	-1.0 %	1.0 %
1.02	0.974	0.6 %	-0.1 %	1.7 %
1.05	0.941	0.7 %	0.6 %	2.2 %

As Table 4 and Table 5 show, VLM is least accurate to predict the propeller's thrust but most accurate to predict the propeller's torque. This is due to the fact that VORTEX uses a friction correction mechanism that can be adapted by measurements, which naturally has been done for the PPTC. BEM and FVM are on the same accuracy level with FVM having the edge but deteriorating in accuracy towards higher advance ratios which is most likely an effect of the compromise mesh suitable for a broad range of advance ratios. Nevertheless, the highest accuracy in cavitation prediction is expected from FVM, followed by BEM and finally VLM.

4 CAVITATION PREDICTION

As stated previously, the cavitation test of the PPTC 2011 itself does not match with FVM calculations regarding cavitation so this evaluation compares the results of each method to the result of a two-phase LES which is deemed sufficiently accurate.

Three cavitation phenomena can be observed at the blade, as shown in Figure 3. There is cavitation on the leading edge of the blade's suction side stretching to the blade tip where a cavitating vortex originates. The blade root also shows cavitation.

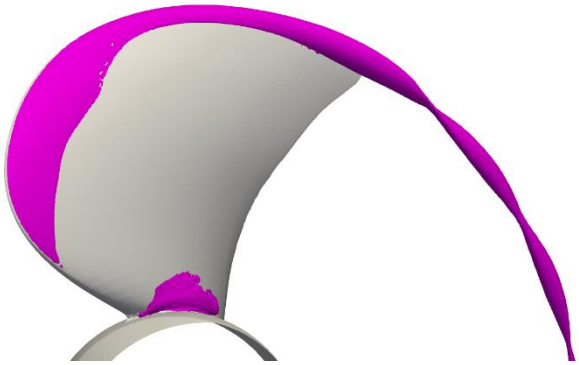

Figure 3 Cavitation prediction by two-phase LES

4.1 Homogenous Inflow

Although a homogenous inflow implies no local modification of the operation point and thus a wake field with axial component = 1 and no tangential and radial component, the interpolation component of the method is still relied upon to evaluate the cavitation at an arbitrary operation point. The homogenous inflow condition is therefore ideally suited to assess the validity of the interpolation isolated from wake field specific effects.

4.1.1 Results

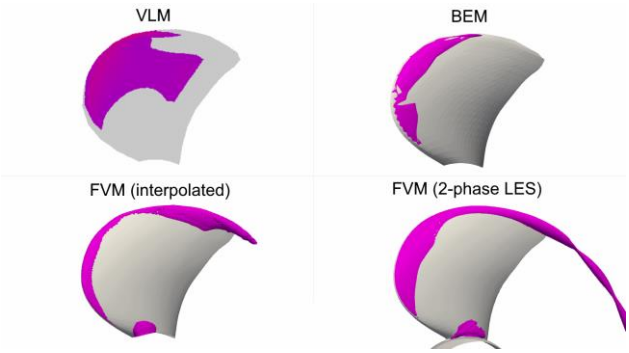

Figure 4 Comparison of different cavitation prediction methods

Figure 4 shows the comparison of the discussed methods. The two-phase LES gives the most detailed prediction, as expected. The BEM as well as the interpolated FVM (the new method presented in this paper) show a comparable amount of leading edge cavitation on the suction side of the blade. Although VLM also shows leading edge cavitation, the propagation of cavitation over the blade surface is much more pronounced than with any other method. VLM and BEM are not able to predict a cavitating tip vortex because that is not supported in the used software at the time of writing. BEM shows a miniscule amount of blade root cavitation, too little to register visually on the image, whereas interpolated FVM gives a fairly accurate impression of this phenomenon.

4.1.2 Different Interpolation Meshes

As described in section 2.2.5 there are different mesh subsets that can be used for the interpolation method. The results obtained for each of these subsets are compared to the two-phase LES in Figure 5.

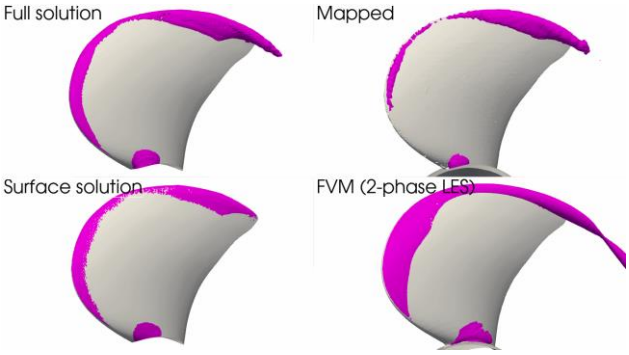

Figure 5 Comparison of different interpolation bases

It is apparent that using the full solution (although most certainly incorrect in the far field) yields results closest to the two-phase LES calculation, with a pronounced start of a tip vortex and sizable blade root cavitation. The surface solution differs only slightly, because it was obtained as a surface export directly from the full solution. Being only the surface representation though, it cannot give any information about the volumetric extent of the cavitation and thus does not show the tip vortex. For the mapped result, the full result was transferred to a smaller mesh with no surface layers. It still shows some cavitation on the leading edge and retains information about the tip vortex. Nevertheless, a degradation of resolution and accuracy is apparent, so the smaller mesh should be designed with care.

4.1.3 Performance Evaluation

Calculation times for this specific case are given in Table 6 and reflect the reason for developing the method presented in this paper.

Table 6 Comparison of calculation times

	Calculation time	Calculation time per cavitation prediction
VLM	1 min	1 min
BEM		1 h
FVM	4 h per advance ratio. Scales according to hardware availability	1 h full solution, 10 min mapped solution, 5 min blade surface only
Two phase LES		1 week on 100 cores (around $12 \cdot 10^6$ to $20 \cdot 10^6$ cells, depending on resolution of tip vortex)

Although the set of calculations needed for the interpolation method takes a relatively long time to compute, it is offset by the gains in accuracy and generality of the solution. Not only is the open water performance of the propeller design evaluated, but it serves as a basis for a multitude of evaluations of different operation points. Compared to BEM and assuming a suitably mapped solution the purely temporal break-even point is reached at four to five different operation points. Considering the added value of FVM by giving information about a cavitating tip vortex and providing the OWC this break-even will likely come much earlier.

4.2 Inhomogeneous Inflow

The presented interpolation approach shows a good accuracy of cavitation prediction compared to more detailed and advanced methods (e.g. two-phase LES). The next step is to check whether the effect of a wake field is correctly represented. The PPTC 2015 used the same propeller as the PPTC 2011 but the propeller shaft is inclined by 12° which results in very different, inhomogeneous flow conditions.

To construct a wake field for this flow is trivial and easily done, though a slight caveat is that the effect of the hub in oblique flow conditions is not modelled correctly, as the hub acts partly as an obstruction to the flow.

Figure 6 Comparison cavitation observations (SVA Potsdam, 2015) vs. interpolated FVM predition

Figure 6 shows a photograph from the modeltest and the interpolated prediction. A difference in cavitation behaviour can clearly be seen between the upper and lower blade positions. This is reflected in the modeltest and matches with what is expected. Due to issues with intellectual property, no real propellers tested behind a hull can be shown here but experience shows that the approach of evaluating a wake field for each point in the FVM solution and interpolating to the local operation point yields very satisfactory results.

5 CONCLUSIONS

A novel method for an accelerated evaluation of propeller operation points based on finite volume method open water simulations with given wake fields is presented. This method is tested against model test, Vortex-Lattice and Boundary-Element method in homogenous and oblique inflow.

Wake-dependent open water interpolation holds up very well to more accurate methods like 2-phase LES and clearly exceeds the prediction accuracy of VLM and BEM. It offers a very good compromise between calculation time and result accuracy and is thus well suited as part of the propeller design toolchain.

There are some simplifications in the approach that have to be validated or overcome going forward, such as the interaction between propeller and wake field or the best

meshing strategy for the mapping mesh. Additionally, there is potential in this method to be used either on solution fields other than the pressure or for other effects than cavitation such as pressure pulses.

A further future improvement in tip vortex prediction for BEM as presented by Kinnas and Kim (2020) may improve the prediction accuracy of the tip vortex itself without affecting the overall cavitation prediction on the sheet. A downstream processing of the calculated velocity and pressure information for the tip vortex, see Gosda (2021), could improve the accuracy for all presented methods.

REFERENCES

Goldstein, S. (1929), 'On the vortex theory of screw propellers'. Proceedings of The Royal Society A: Mathematical, Physical and Engineering Sciences 123: 440-465.

Gosda, R. (2021). 'Numerische Simulation ausgedehnter Spitzenwirbelkavitation eines Propellers mit einer Randelementmethode mit Relaxationszonen'. https://www.soft-matter.ovgu.de/softmatter_media/Aktuelles/Workshop+Kavitation+2021/Talks/presentation_Gosda_Numerische+Simulation+ausgedehnter+Spitzenwirbelkavitation+eines+Propellers+mit+einer+Randelementmethode+mit+Relaxationszonen.pdf, visited 12th January 2024.

Kimmerl, J.; Mertes, P.; Abdel-Maksoud, M. (2021). 'Application of Large Eddy Simulation to Predict Underwater Noise of Marine Propulsors. Part 1: Cavitation Dynamics'. Journal of Marine Science and Engineering 9 (8) : 792.

Kinnas, A S.; Lee, H.; Young, Yin L. (2003) 'Modeling of Unsteady Sheet Cavitation on Marine Propeller blades'. International Journal of Rotating Machinery 9.

Kinnas, A. S.; Kim, S. (2020). ‚Prediction of Unsteady Developed Tip Vortex Cavitation and Its Effect on the Induced Hull Pressures'. Journal of Marine Science and Engineering 8.

Krasilnikov, V. (2019). 'CFD modelling of hydroacoustic performance of marine propellers: Predicting propeller cavitation'. Numerical Towing Tank Symposium (NuTTS), Portugal.

Mangani, L.; Buchmayr, M.; Darwish, M. (2014). ‚Development of a Novel Fully Coupled Solver in OpenFOAM: Steady-State Incompressible Turbulent Flows in Rotational Reference Frames'. Numerical Heat Transfer, Part B: Fundamentals 66, 6: 526-543.

Schneer, G.; Sauer J. (2001). ‚Physical and Numerical Modeling of Unsteady Cavitation Dynamics'; ICMF-2001, 4th International Conference on Multiphase Flow, New Orleans, USA.

Schulze, R. (1995). ‚Das Propeller-Entwurfs und Optimierungskonzept der SVA'. Jahrbuch der Schiffbautechnischen Gesellschaft 89: 347-353.

SVA Potsdam (2011). 'PPTC'11'. https://www.sva-potsdam.de/pptc-smp11-workshop/, visited 19th October 2023.

SVA Potsdam (2015). 'PPTC'15'. https://www.sva-potsdam.de/smp15-propeller-workshop/, visited 19th October 2023.

Viitanen, V.; Siikonen, T; Sánchez-Caja, A. (2020). ‚Cavitation on Model- and Full-Scale Marine Propellers: Steady and Transient Viscous Flow Simulations at Different Reynolds Numbers'. Journal of Marine Science and Engineering 8 (2).